

Highly accessible catalytic sites on recyclable organosilane-functionalized magnetic nanoparticles: An alternative to functionalized porous silica catalysts

Nam T. S. Phan, Christopher W. Jones*

School of Chemical & Biomolecular Engineering, Georgia Institute of Technology, 311 Ferst Dr., Atlanta, GA 30332, USA

Received 19 January 2006; received in revised form 11 March 2006; accepted 13 March 2006

Available online 2 May 2006

Abstract

Diaminosilane-functionalized cobalt spinel ferrite (CoFe_2O_4) magnetic nanoparticles are synthesized and used as efficient heterogeneous base catalysts for the Knoevenagel condensation of aromatic and heteroaromatic aldehydes with malononitrile. The magnetic nanoparticle catalyst is characterized by X-ray powder diffraction (XRD), transmission electron microscopy (TEM), thermogravimetric analysis (TGA), Fourier transform infrared (FTIR), and nitrogen physisorption measurements. Quantitative conversion of the reactants is achieved under mild conditions. Recovery of the catalyst is easily achieved by magnetic decantation. The supported catalyst is reused five times without significant degradation in catalytic activity. No contribution from homogeneous catalysis due to active amine species leaching into reaction solution is detected. The performance of the magnetic base catalyst in the Knoevenagel reaction is directly compared with diamine-functionalized SBA-15 and MCM-48. Reaction rates over the non-porous, magnetic nanoparticle catalyst are comparable to the large pore mesoporous silica materials and faster than the small pore MCM-48 material with ~ 22 Å diameter pores. A significant effect of the acidity of the magnetic nanoparticle support on catalyst activity in the Knoevenagel condensation is also observed.

© 2006 Elsevier B.V. All rights reserved.

Keywords: Knoevenagel condensation; Nanoparticle; Magnetic separation; Base catalyst

1. Introduction

The immobilization of homogeneous catalysts to facilitate easy catalyst recovery and recycling, as well as product separation, is a longstanding pursuit of catalysis science [1]. Various support matrices such as organic polymers and inorganic silica, especially porous inorganic materials with high surface areas, have been employed [2–4]. However, a substantial decrease in activity of the immobilized catalyst is commonly observed, especially under low temperature liquid phase conditions, due to the problem of reactant diffusion to the surface-anchored catalyst [5]. Nanoparticles have emerged as efficient alternative support materials for homogeneous catalyst immobilization [6]. When the size of the support material is decreased to the nanometer scale, high surface areas can be obtained, with all of the area on the external surface of the particle when non-

porous nanoparticles are used. As a consequence, the activity of nanoparticle-supported catalysts could be improved compared to homogeneous catalysts immobilized on conventional, porous support matrices under conditions where internal pore diffusion can represent a rate limiting step. However, in this case, facile separation and recycling of nanoparticle materials from reaction media still remains a challenge, as they are often colloidal and therefore easily dispersed in liquid media by Brownian motion. This issue can be addressed by using magnetic supports, allowing the catalyst to be easily separated from the liquid reaction media with application of an external magnetic field. Recently, we demonstrated that the combination of functionalized, superparamagnetic nanoparticles with traditional gravimetrically recovered catalysts allows for the promotion of one-pot, multi-step catalytic reactions with complete recovery of the various catalysts in pure form [7]. The synthesis and use of superparamagnetic nanoparticles such as spinel ferrite nanoparticles has been intensively investigated over the last few years due to their tunable magnetic properties [8,9]. In the field of catalysis, magnetic nanoparticles have recently

* Corresponding author. Tel.: +1 404 385 1683; fax: +1 404 894 2866.
E-mail address: cjones@chbe.gatech.edu (C.W. Jones).

been utilized as catalyst supports for organic transformations such as olefin hydroformylation [10], nitrobenzene hydrogenation [11], olefin hydrogenation [12], Suzuki cross-coupling [13], asymmetric hydrogenation [14], and biocatalytic transformations [15].

The Knoevenagel condensation of aldehydes with compounds containing activated methylene groups is one of the most useful and widely employed methods for carbon–carbon bond formation with numerous applications in the synthesis of fine chemicals [16] as well as heterocyclic compounds of biological significance [17]. Conventionally, this reaction is catalyzed by weak bases like primary, secondary, and tertiary amines under homogeneous conditions, which often requires upwards of 40 mol% catalyst with the attendant difficulties in catalyst recovery and recycling [18]. Over the last decades, various solid-supported catalysts have been applied to this reaction such as aminoalkylsilane functionalized silica [19], tetraalkylammonium hydroxide-immobilized MCM-41 [20], guanidine-immobilized MCM-41 or SBA-15 [21,22], ammonia-grafted FSM-16 [23], ammonia-treated zeolites [24], basic metal-exchanged zeolites [25], MCM-48 with silicon oxynitride frameworks [26], and silicate-organic composite materials [27]. Additionally, Knoevenagel reactions catalyzed by Lewis acids have also been reported [28,29].

As noted above, we recently demonstrated a combination of catalysts recovered by magnetic, gravimetric, and membrane methods in multi-step, one-pot reactions with recovery of each individual catalyst [7]. In this work, we wish to report the utilization of diamine-functionalized superparamagnetic spinel ferrite nanoparticles as efficient heterogeneous catalysts for low temperature liquid phase reactions with, in principle, no rate contribution associated with internal diffusional resistances. The Knoevenagel reaction of malononitrile with aromatic and heteroaromatic aldehydes is utilized as a well-known model reaction under very mild conditions. High activity is observed and the magnetic catalyst is easily isolated from the reaction mixture by simple magnetic decantation and reused without significant degradation in activity. The performance of the magnetic base catalyst in the Knoevenagel reaction is directly compared with diamine-functionalized hexagonal mesoporous SBA-15 materials of different pore diameters and cubic mesoporous MCM-48 as typical porous silica catalysts that represent a current benchmark in low temperature, liquid phase fine chemical catalysis.

2. Experimental

2.1. Materials and instrumentation

Cobalt(II) chloride (Alfa Aesar, anhydrous, 99.5%), iron(II) chloride (Alfa Aesar, anhydrous, 99.5%), acetone (Acros, 99%), ammonium hydroxide (Fisher, 29%, v/v, aqueous solution), benzaldehyde (Aldrich, anhydrous, 99%), benzene (Aldrich, anhydrous, 99%), 4-chlorobenzaldehyde (Acros, 98%), ethanol (Fisher, 99%), 2-furaldehyde (Acros, 99%), *n*-hexadecyltrimethylammonium (Aldrich), hexamethyldisilazane (HMDS) (Aldrich, 99%), hexanes (Fisher, 99%), hydrochloric acid (HCl) (JT Baker; A.C.S. Reagent), malononitrile (Acros,

99%), 2-hydroxybenzaldehyde (Acros, 99%), 4-hydroxybenzaldehyde (Acros, 99%), methanol (Acros, anhydrous, 99%), methylamine (Alfa Aesar, 40%, w/w, aqueous solution), 4-methoxybenzaldehyde (Acros, 99%), 4-methylbenzaldehyde (Acros, 97%), 4-nitrobenzaldehyde (Acros, 99%), poly(ethylene glycol)-*block*-poly(propylene glycol)-*block*-poly(ethylene glycol) (EO-PO-EO) (Aldrich), *N*-propylethylenediamine (Acros, 99%), 2-pyridinecarboxaldehyde (Acros, 99%), 4-pyridinecarboxaldehyde (Acros, 98%), pyrrole-2-carboxaldehyde (Acros, 99%), sodium dodecyl sulfate (Acros, 85%), tetraethyl orthosilicate (TEOS; Acros, 98%), *N*-[3-(trimethoxysilyl)propyl]ethylenediamine (Acros, 99%), 1,3,5-trimethylbenzene (TMB) (Aldrich, 97%), and *o*-xylene (Acros, 99%) were used as received. Ethyl acetate (Fisher, 99%) and tetrahydrofuran (THF) (Fisher, 99%) were dried over 4 Å molecular sieves. Deionized water was purged with nitrogen overnight prior to use.

A Fischer Scientific FS60H (low wattage sonication bath) was used to sonicate samples. Nitrogen physisorption measurements were conducted using a Micromeritics ASAP 2010 system. Samples were pretreated by heating under vacuum at 150 °C overnight. The surface areas were analyzed by the BET method, and the pore size distribution was determined using the BJH method applied to the adsorption branch of the isotherm. A Netzsch Thermoanalyzer STA 409 was used for simultaneous thermogravimetric analysis (TGA) and differential scanning calorimetry (DSC) with a heating rate of 10 °C/min in air. X-ray powder diffraction (XRD) patterns were recorded using Cu K α radiation source on a Scintag X1 powder diffractometer. Transmission electron microscopy studies were performed using a JEOL 100CX II transmission electron microscope (TEM) at 100 kV and 100,000 magnification. The nanoparticles were dispersed on holey carbon grids for TEM observation. Fourier transform infrared (FTIR) spectra were obtained on a Bruker IFS 66 V/S instrument in transmission mode with samples being dispersed in potassium bromide pellets. Gas chromatographic (GC) analyses were performed using a Shimadzu GC 14-A equipped with a flame ionization detector (FID) and an HP-5 column (length = 30 m, inner diameter = 0.25 mm, and film thickness = 0.25 μ m). The temperature program for GC analysis heated samples from 50 to 140 °C at 30 °C/min, from 140 to 300 °C at 40 °C/min, and held at 300 °C for 2 min. Inlet and detector temperatures were set constant at 330 °C. *o*-Xylene was used as an internal standard to calculate the reaction conversion. GC-MS analyses were performed using a Hewlett Packard GC-MS 5890 with a DB-5 column (length = 30 m, inner diameter = 0.25 mm, and film thickness = 0.25 μ m). The temperature program heated samples from 30 to 300 °C at 15 °C/min and held at 300 °C for 5 min.

2.2. Synthesis of magnetic nanoparticles

Cobalt spinel ferrite (CoFe₂O₄) nanoparticles were synthesized following a microemulsion method [30]. Cobalt(II) chloride (0.9 g, 6.9 mmol) and iron(II) chloride (1.9 g, 14.9 mmol) were mixed in an aqueous solution (500 ml). An aqueous surfactant solution of sodium dodecyl sulfate (SDS) (12.9 g,

38.3 mmol) in deionized water (500 ml) was added, and the mixture was stirred at room temperature for 30 min to form a mixed micellar solution of Co(II) dodecyl sulfate and Fe(II) dodecyl sulfate. The mixture was then heated to 55–65 °C. A solution of methylamine (300 ml, 40%, w/w, aqueous solution) in deionized water (700 ml) was heated to the same temperature and rapidly added to the surfactant mixture. Black nanoparticles were precipitated. After the reaction mixture was stirred vigorously for 3 h, the nanoparticles were isolated by centrifugation and washed with copious amounts of deionized water, ethanol, and hexanes. The final product was dried in air at 50 °C overnight to yield superparamagnetic cobalt spinel ferrite nanoparticles (1.7 g).

2.3. Amino-functionalized magnetic nanoparticles

The magnetic nanoparticles were functionalized with *N*-[3-(trimethoxysilyl)propyl]ethylenediamine according to a slightly modified reported procedure [31]. CoFe₂O₄ nanoparticles (1.1 g) were dispersed in a mixture of ethanol and water (150 ml, 1:1, v/v). The suspension was sonicated for 30 min at room temperature. Ammonium hydroxide (15 ml, 29%, v/v, aqueous solution) was added, and the mixture was stirred vigorously at 60 °C for 24 h under an argon atmosphere. The nanoparticles were washed with copious amounts of deionized water, ethanol, and hexanes via magnetic decantation. Details of the magnetic decantation method are provided in Section 2.6. The resulting product was redispersed in a mixture of ethanol and water (150 ml, 1:1, v/v), and sonicated for 30 min at room temperature. *N*-[3-(Trimethoxysilyl)propyl]ethylenediamine (1 g) was then added, and the solution was heated at 60 °C with vigorous stirring for 24 h under an argon atmosphere. The final product was washed with copious amounts of deionized water, ethanol, and hexanes by magnetic decantation, and dried under vacuum at room temperature overnight to yield amino-functionalized magnetic nanoparticles (1.1 g). Capping the remaining surface hydroxyl groups was achieved by stirring a portion of the as-synthesized materials (40 mg) with a large excess of hexamethyldisilazane (50 mg) in toluene (5 ml) at room temperature overnight. The final product was washed with copious amounts of toluene, ethanol, and hexanes by magnetic decantation, and dried under vacuum at room temperature overnight.

2.4. Synthesis of SBA-15 and amino-functionalized SBA-15

Large pore SBA-15 (100 Å) was synthesized by literature methods, utilizing the triblock poly(ethylene oxide)–poly(propylene oxide)–poly(ethylene oxide) non-ionic surfactant as the structure-directing agent and 1,3,5-trimethylbenzene as a swelling cosolvent [32]. Small pore SBA-15 (65 Å) was synthesized using a similar procedure except no swelling cosolvent was employed. The as-prepared material was calcined using the following temperature program: (1) increasing the temperature (1.2 °C/min) to 200 °C, (2) heating at 200 °C for 1 h, (3) increasing the temperature (1.2 °C/min) to 550 °C, and (4) holding at 550 °C for 6 h. Prior to functionalization, the SBA-15 was dried under vacuum at 200 °C for 3 h and stored in a dry box. Amino-functionalized SBA-15 was synthesized by

stirring a toluene (30 ml) suspension of SBA-15 (1 g) and *N*-[3-(trimethoxysilyl)propyl]ethylenediamine (1 g) at room temperature for 24 h under an argon atmosphere. The solid was then filtered and washed with copious amounts of toluene, hexanes, methanol, and diethyl ether in a dry box and dried under vacuum at room temperature overnight, yielding approximately 1 g of amino-functionalized SBA-15.

2.5. Synthesis of MCM-48 and amino-functionalized MCM-48

MCM-48 was synthesized by literature methods, utilizing tetraethyl orthosilicate (TEOS) as silica source, *n*-hexadecyltrimethylammonium as template, ethanol as solvent, water as a reactant, and ammonia as catalyst for the hydrolysis and condensation of the silica source [33]. The as-prepared material was calcined using the temperature program as described above. Prior to functionalization, the MCM-48 was dried under vacuum at 200 °C for 3 h and stored in a dry box. Amino-functionalized MCM-48 was synthesized by stirring a toluene (5 ml) suspension of MCM-48 (0.2 g) and *N*-[3-(trimethoxysilyl)propyl]ethylenediamine (0.2 g) at room temperature for 30 h under an argon atmosphere. The solid was then filtered and washed with copious amounts of toluene, hexanes, methanol, and ether in a dry box and dried under vacuum at room temperature overnight.

2.6. Catalytic studies

Unless otherwise stated, a mixture of basic magnetic nanoparticles (33 mg, 2.5 mol%), benzaldehyde (40 mg, 0.38 mmol), and *o*-xylene (21 mg, 0.2 mmol) in benzene (3 ml) was placed into a 10 ml glass vessel. The reaction vessel was sonicated for 5 min at room temperature to disperse the magnetic nanoparticles in solution. A solution of malononitrile (49 mg, 0.75 mmol) in benzene (1 ml) was then added, and the resulting mixture was stirred at room temperature under an argon atmosphere. Reaction conversion was monitored by withdrawing aliquots from the reaction mixture at different time intervals, quenching with acetone, filtering through a short silica gel pad, analyzing by GC with reference to *o*-xylene, and further confirming product identity by GC–MS. After quantitative conversion was achieved, an external magnetic field was applied on the outer surface of the glass reaction vessel containing the magnetic nanoparticles and the reaction solution. The solution was removed from the reaction vessel by decantation while the external magnet held the basic nanoparticles stationary inside the vessel. The nanoparticles were then washed with anhydrous benzene, separated by magnetic decantation as described above, dried under vacuum overnight at room temperature, and reused if necessary. For the leaching test, fresh reagents were added to the separated reaction solution, and the resulting mixture was stirred at room temperature for 180 min. Reaction progress, if any, was monitored by GC as previously described. The reaction was also carried out using different catalyst loadings, different solvents, and different aromatic aldehydes, respectively. Diamine-functionalized SBA-15 and MCM-48 were used as silica-based

catalysts in the reaction, for comparison with the basic magnetic catalyst.

3. Results and discussion

3.1. Catalyst synthesis and characterization

Cobalt spinel ferrite nanoparticles were synthesized following a microemulsion method [30]. It was previously reported that magnetic nanoparticles synthesized in basic aqueous media are covered with a number of surface hydroxyl (–OH) groups [34]. The hydroxyl groups on the surface of the magnetic nanoparticles were then enriched with an aqueous solution of ammonia, facilitating the surface modification step. The resulting nanoparticles were functionalized via silane chemistry with *N*-[3-(trimethoxysilyl)propyl]ethylenediamine to create surface base sites, according to a slightly modified literature procedure [31]. It was decided to immobilize diamine species on the nanoparticle surface as the diamine exhibited high activity in the Knoevenagel condensation under mild conditions, either in sol–gel entrapped form [35] or silica supported form previously [36].

SBA-15 has emerged as one of the most commonly used mesoporous silica catalyst supports [37]. It is known to be a well-defined, hexagonal mesoporous silica material with straight mesopores that are connected through small micropores. Mesoporous silicas of this type are useful model supports, as they are highly ordered, hydrothermally stable, and have pores of low polydispersity [37]. In particular, guanidine moiety-functionalized SBA-15 was found highly active towards the Knoevenagel reaction [22]. In the current contribution, an SBA-15 supported diamine catalyst was synthesized using a method we previously reported [38], substituting *N*-[3-(trimethoxysilyl)propyl]ethylenediamine for 3-aminopropyltrimethoxysilane, and used as a benchmark porous catalyst for

comparison to the basic magnetic nanoparticle catalyst in the Knoevenagel condensation. Furthermore, mesoporous MCM-48 with a smaller pore size than the SBA-15 materials was also functionalized with the diamine moiety and used to study the effect that mass transfer (internal diffusion) might have on the reaction rate of the heterogeneous Knoevenagel condensation.

The amino-functionalized superparamagnetic nanoparticles were characterized using a variety of different techniques. X-ray powder diffraction showed that the magnetic nanoparticles are spinel ferrites, with XRD patterns being consistent with literature (Fig. 1) [30]. No other crystalline phases were observed in the XRD diffractogram. Thermogravimetric analysis of the supported catalyst showed that approximately 0.3 mmol/g of the diamine was immobilized on the ferrite nanoparticles. Transmission electron microscopy studies showed an average diameter of approximately 30 nm for the particles (Fig. 2). Particle agglomeration was clearly observed for the unmodified nanoparticles, and the primary particle size is likely closer to 10 nm in diameter. Indeed, nitrogen physisorption measurements of the nanoparticles gave BET surface areas of 200 m²/g and no measurable mesoporosity. The high surface area in conjunction with the lack of mesoporosity indicates that the primary particle size of the nanoparticles is much smaller than the observed 30 nm observed in the TEM images. Simple surface area calculations assuming non-porous, spherical particles indicate that a surface area of 200 m²/g corresponds to a primary particle size of ~6 nm diameter. In the TEM images, a slight agglomeration was also observed for the amino-functionalized ferrite nanoparticles, though it was less pronounced. It was inferred that the amine groups of the silane coated on the surfaces reduce the aggregation of the ferrite nanoparticles. This would agree with the observations of Liang and co-workers, where magnetite nanoparticles (Fe₃O₄) were coated with 3-aminopropyltriethoxysilane [31]. It should be noted that most oxide particles, regardless of composition, aggregate on TEM grids and the images do not

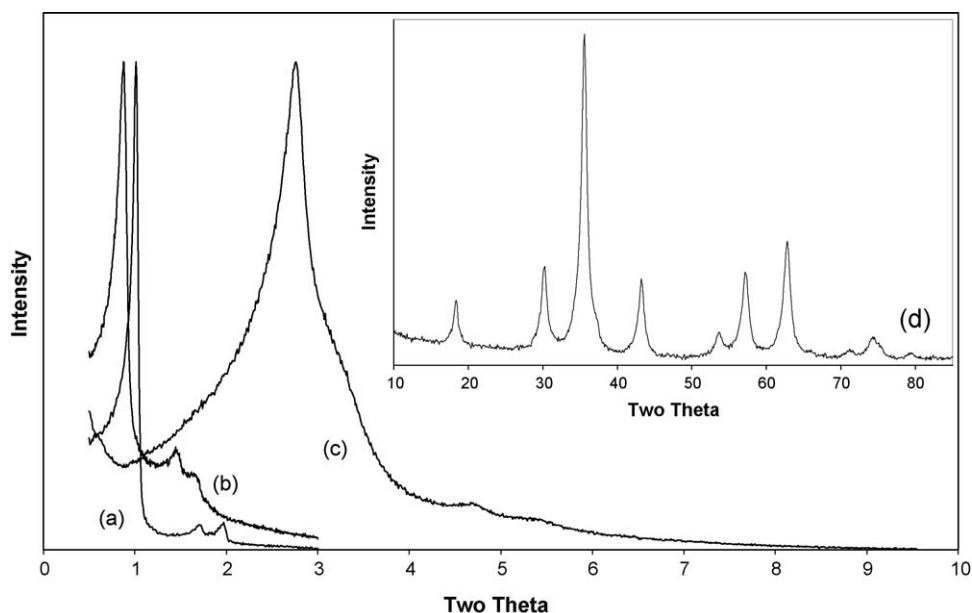


Fig. 1. X-ray powder diffractogram of different catalysts: small pore SBA-15 (a), large pore SBA-15 (b), MCM-48 (c), and magnetic nanoparticles (d).

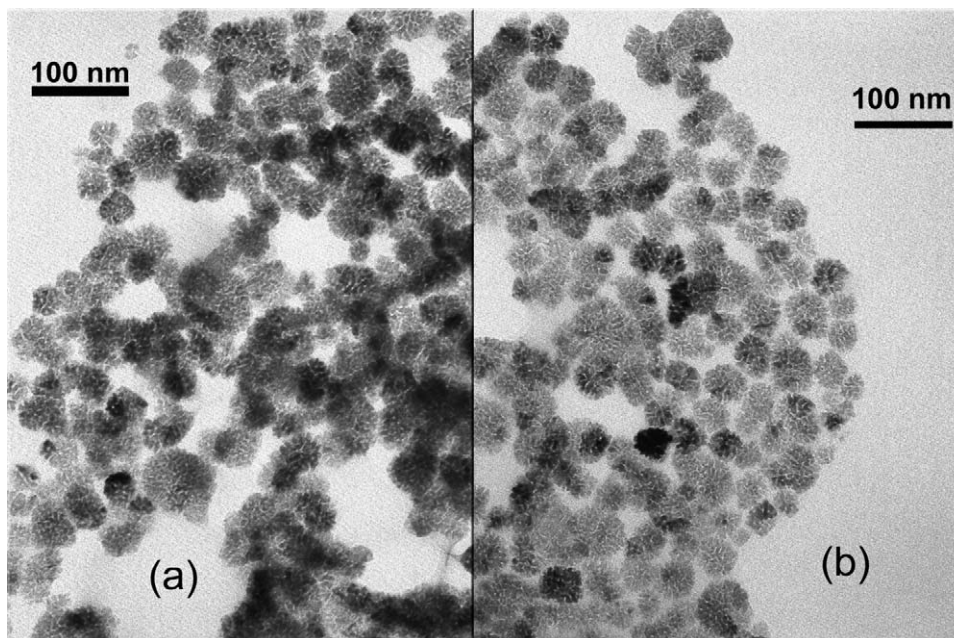


Fig. 2. TEM micrograph of the unfunctionalized (a) and amino-functionalized (b) magnetic nanoparticles.

imply that the nanoparticles necessarily aggregate similarly in solution.

Fourier transform infrared spectra of both the unfunctionalized and amino-functionalized nanoparticles showed the presence of an Fe–O stretching vibration at approximately 595 cm^{-1} , an O–H stretching vibration due to physisorbed water and potentially surface hydroxyls near 3420 cm^{-1} , and an O–H deformation vibration near 1630 cm^{-1} , respectively (Fig. 3) [31,34]. The significant features observed for the diamine-functionalized nanoparticles are the appearance of the peaks at 1017 cm^{-1} (Si–O stretching), and 2920 cm^{-1} ($-\text{CH}_2$ stretching). There also exists the contribution of the $-\text{NH}_2$ group for the band near 3300 cm^{-1} , which is overlapped by the O–H stretching vibration. These features revealed the existence of the aminosilane

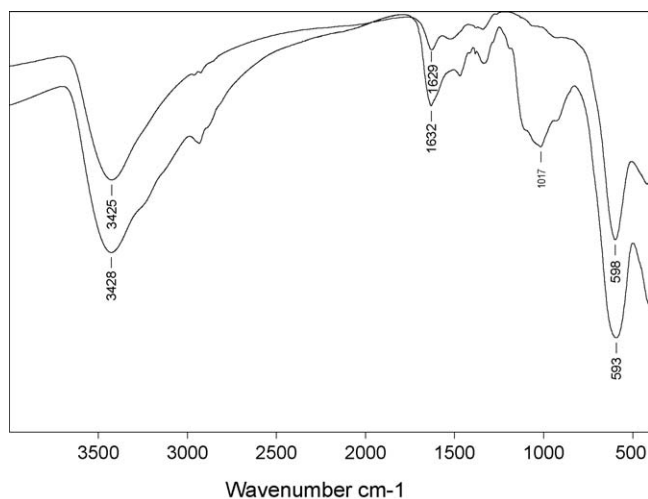


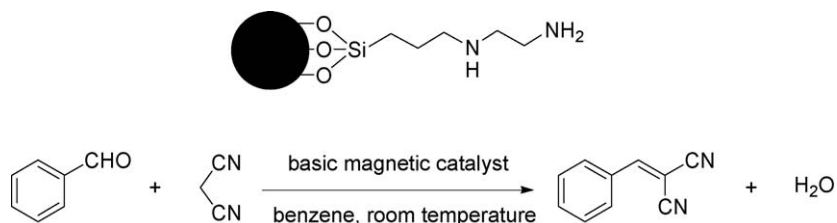
Fig. 3. FTIR spectra of unfunctionalized (top) and amino-functionalized (bottom) magnetic nanoparticles.

species on the particles, and the spectrum is in good agreement with literature [31].

XRD was also used to determine the structural order of the SBA-15 and MCM-48 materials. The XRD patterns of the SBA-15 (Fig. 1) are in good agreement with a hexagonal pore structure [37]. The XRD patterns of the MCM-48 (Fig. 1) are also consistent with literature [39]. The large pore SBA-15 used in this study has an average mesopore size of 101 \AA and a BET surface area of $960\text{ m}^2/\text{g}$ on the basis of low-temperature nitrogen physisorption measurements. An average mesopore size of 65 \AA and a surface area of $930\text{ m}^2/\text{g}$ were observed for the medium pore SBA-15. The presence of a higher surface area for the material with larger mesopores is a consequence of different amounts of microporosity in the two samples [40]. Low-temperature nitrogen physisorption measurements of the MCM-48 used in this contribution showed an average mesopore size of 22 \AA and a BET surface area of $1490\text{ m}^2/\text{g}$. The TGA of the amino-functionalized SBA-15 catalysts revealed that approximately 1.2 mmol/g of the diamine were immobilized onto the silica supports (both 65 and 100 \AA SBA-15). Similarly, a loading of 1.3 mmol/g of the diamine was observed for the amino-functionalized MCM-48 catalyst.

3.2. Catalytic studies

The magnetic nanoparticle-supported diamine catalyst was assessed for its activity in the Knoevenagel reaction by studying the condensation of benzaldehyde with malononitrile to form benzylidene malononitrile as the principal product (Scheme 1). The initial reaction was carried out using $2.5\text{ mol}\%$ magnetic catalyst relative to benzaldehyde in benzene at reflux temperature [35]. Complete conversion was achieved within just 5 min with no trace amount of benzaldehyde being detected by GC.



Scheme 1. Knoevenagel reaction of benzaldehyde with malononitrile using basic magnetic nanoparticle catalyst.

It was therefore decided to carry out the reaction under milder conditions (i.e. room temperature). The catalyst concentration, with respect to the diamine moiety immobilized on the magnetic nanoparticles, was studied in the range of 0.5–2.5 mol% at room temperature. Aliquots were withdrawn from the reaction mixture at different time intervals and analyzed by GC, giving kinetic data during the course of the reaction. Experimental results are summarized in Fig. 4. Quantitative conversion of benzaldehyde was achieved in just 20 min at 2.5 mol% catalyst loading. As expected, decreasing the catalyst loading resulted in a drop in reaction rate, with complete conversion being observed within 75 min at 1.5 mol% catalyst loading (however, initial TOFs are approximately the same in all cases $\sim 2\text{--}3\text{ min}^{-1}$). Reaction using 0.5 mol% catalyst still afforded a quantitative yield, although a longer reaction time was required to convert all of the benzaldehyde to the desired product (4 h). The results indicated that the diamine-functionalized magnetic nanoparticles were quite active in the Knoevenagel reaction. Furthermore, the reaction rate observed for the basic magnetic catalyst appears higher than some previously reported catalysts, where longer reaction time or/and higher catalyst loadings were required for the same reaction (although in these cases no kinetic data were provided, and only conversion at the end of the experiment was reported) [27,41].

It should be noted that the unfunctionalized magnetic nanoparticles were only very weakly active in the Knoevenagel condensation, with less than 5% conversion observed within

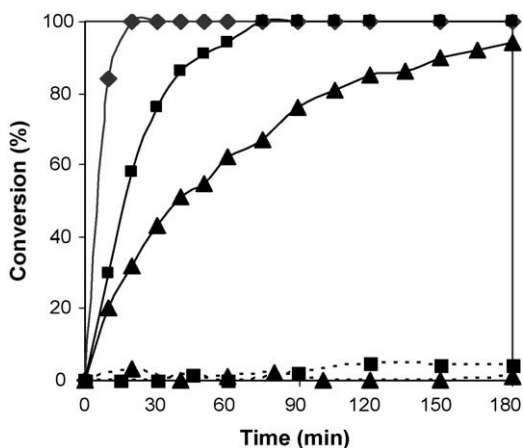


Fig. 4. Effect of catalyst concentration. Diamonds, squares, and triangles represent kinetic data for reactions using 2.5, 1.5, and 0.5 mol% catalyst, respectively. Broken lines show the leaching test result (triangles) and kinetics of the control reaction using unfunctionalized magnetic nanoparticles (squares). All reactions were at room temperature.

3 h (Fig. 4). This indicated the necessity of the diamine coating on the surface of the magnetic nanoparticles to create basic sites. When using a supported catalyst, a crucial issue is the possibility that some of active sites could migrate from the solid support to the liquid phase and that these leached species could become responsible for a significant part of the catalytic activity. In order to determine if leaching was a problem, an experiment was performed to estimate the contribution of leached active species to the catalytic activity. After the reaction, the basic magnetic catalyst was separated from the reaction mixture by magnetic decantation under a permanent magnetic field. The reaction solution was transferred to a new reactor vessel, and fresh reagents were then added to the solution. The resulting mixture was stirred for 3 h at room temperature with aliquots being sampled at different time intervals, and analyzed by GC. The data from GC determinations gave quantitative information about residual, catalytically active amine in solution. Within experimental error, no further reaction was observed, indicating there was no contribution from leached active species (Fig. 4). It was therefore inferred that the active amine moiety was retained on the solid support during the course of the reaction.

The sensitivity of a heterogeneously catalyzed reaction to different solvents can usually be of extreme importance, depending on the nature of the catalyst support material [42,43]. Macquarrie et al. previously reported that the Knoevenagel condensation using silica supported catalysts had a very limited range of effective solvents, and gave the best reaction rate in non-polar solvents [42,44]. We therefore decided to investigate the solvent effect in the basic magnetic nanoparticle-catalyzed reaction, using 1.5 mol% catalyst loading at room temperature. As mentioned previously, benzene is one of the solvents of choice for the Knoevenagel reaction. In this work, a combination of benzene and the basic magnetic catalyst afforded excellent conversions for the reaction within a short reaction time (Fig. 5). The reaction carried out in THF, a relatively polar solvent, also gave a similar reaction rate with all of the benzaldehyde being converted to the desired product within 75 min. Interestingly, the basic magnetic catalyst was also reactive in ethyl acetate, although a slight drop in reaction rate was observed, compared to the reaction in benzene (Fig. 5). This is in contrast with the result of Macquarrie and Jackson where the Knoevenagel reaction using aminopropylated MCM catalyst in ethyl acetate was almost ineffective while reactions in non-polar solvents afforded complete conversion, though different reactants were used [44]. It was previously proposed that the rate of the Knoevenagel reaction using silica-based catalysts was influenced by the partitioning of the reactants (polar) between the catalyst pores and/or surface

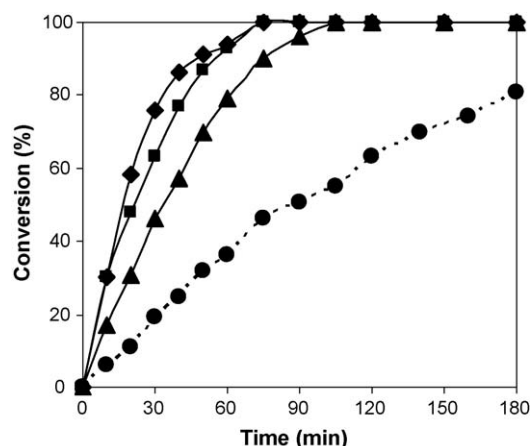


Fig. 5. Knoevenagel reactions in different solvents. Diamonds, squares, and triangles represent kinetic data for reactions in benzene, THF, and ethyl acetate, respectively. Broken lines show kinetic data for the reaction using hydrophobic (capped) magnetic catalyst in ethyl acetate.

(polar) and the bulk reaction media (i.e. partitioning away from the catalyst pores/surface) was increased with more polar solvents [42,44]. The similar trend in the effect of solvent polarity (i.e. more polar solvents are disadvantageous) observed for the magnetic nanoparticle catalyst in this study could be rationalized based on the same factors.

Katz and co-workers [45] investigated the effect of outer-sphere acidity on chemical reactivity of amino-functionalized silica catalysts in the Knoevenagel reaction and indicated that differences between hydrophilic and hydrophobic silica supports resulted in significant effects on the reaction. A higher reaction rate was observed for hydrophilic silica supported catalyst with free acidic silanol groups surrounding the diamine species. Capping the acidic silanol groups resulted in a significant drop in reaction rate. As mentioned previously, the amino-functionalized magnetic nanoparticles were covered with a number of acidic hydroxyl ($-OH$) groups, which may lead to similar effects. It was therefore decided to study the differences in activity between hydrophilic and hydrophobic magnetic nanoparticle supports in the Knoevenagel condensation. The reaction was carried out in ethyl acetate using 1.5 mol% catalyst concentration of the hydrophobic magnetic catalyst, where free acidic hydroxyl groups surrounding the diamine species were capped with methyl groups. As shown in Fig. 5, there was a large difference in activity of the hydrophilic and the hydrophobic magnetic nanoparticle catalysts. A significant drop in reaction rate was observed for the hydrophobic catalyst under identical reaction conditions, which is consistent with the results of Katz and co-workers for amino-functionalized silica catalysts [45]. It was proposed that hydrophilic supports could preactivate the reagents by interaction of the carbonyl groups with the acidic hydroxyl groups, affording reaction rate enhancement [45,46]. Indeed, rate enhancement by using acid–base bifunctional catalysts was also observed for other base-catalyzed reactions such as aldol or nitroaldol condensations, in which the carbonyl groups were also preactivated by the acidic sites prior to the base-catalyzed step [47]. In parallel with the above-mentioned bifunctional effect, the rate enhancement observed

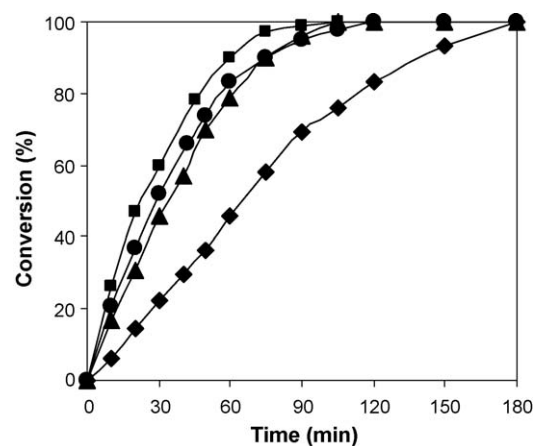


Fig. 6. Effect of catalyst support on reaction rate in ethyl acetate: magnetic nanoparticles (triangles), large pore SBA-15 (squares), small pore SBA-15 (circles), and MCM-48 (diamonds).

for hydrophilic supports could be further enhanced by reactant partitioning, where partitioning away of the reagents (polar) from catalytic sites would be decreased with more polar catalyst supports.

With these results in hand, we then investigated the effect of the catalyst support materials on reaction rate, using different silica supports. Hydrophilic large pore diamine-functionalized SBA-15 (100 Å) was initially used as a typical, state-of-the-art porous silica catalyst for the reaction under identical conditions as compared to the basic magnetic nanoparticle-catalyzed reaction. The reaction was also carried out using hydrophilic small pore SBA-15 (65 Å) and MCM-48 (22 Å) supported catalysts with free acidic silanol groups surrounding the diamine species under the same conditions. In both cases where hydrophilic large pore and small pore SBA-15 supports were employed, the reaction rate was similar to but slightly higher than that of the basic magnetic nanoparticle-catalyzed reaction under the same conditions (Fig. 6). In principle, the rate for the non-porous catalyst should be equal to or higher than that of a porous system under conditions where porosity might influence observed reaction rates. This was not quite achieved in this case, and it suggests that some interparticle interactions leading to clustering may occur for the magnetic nanoparticle catalyst [48], reducing the effective surface area of the catalyst. The possibility of clustering is supported by the TEM images in Fig. 2. Thus, higher rates may be achievable with optimized nanoparticle catalysts. It was further found that the rate of the basic porous silica-catalyzed Knoevenagel reaction was affected by the pore size of the silica supports, as shown in Fig. 6. The reaction rate over large pore (100 Å) SBA-15 catalyst was slightly higher compared to the small pore (65 Å) SBA-15 catalyst, although complete conversion was observed within 2 h in both cases. As expected, the reaction using the MCM-48 supported catalyst proceeded with slowest rate among the four catalysts, due to its small pore size (22 Å). Overall, the initial reaction rates over both SBA-15 samples and the magnetic nanoparticle catalysts were comparable, whereas the rate over MCM-48 catalyst was markedly slower. The drop in reaction rate over the small pore silica supports

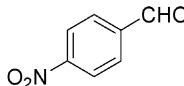
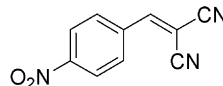
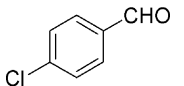
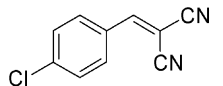
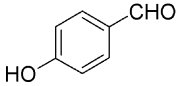
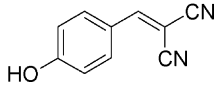
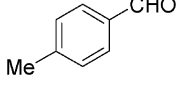
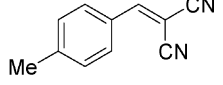
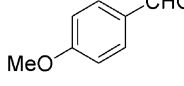
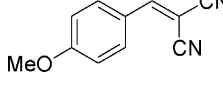
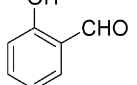
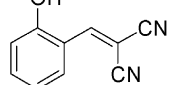
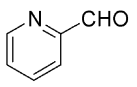
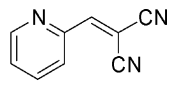
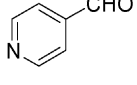
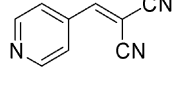
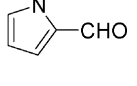
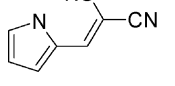
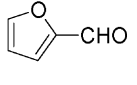
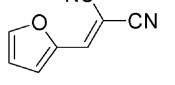
suggests that mass transfer (internal diffusion) influences the reaction rate to a large extent in that case [49].

Another point of great concern for most of anchored catalysts is the ease of separation as well as the deactivation and reusability of the catalyst. The basic magnetic nanoparticle catalyst was therefore investigated for recoverability and reusability over five successive runs. The reaction was carried out in benzene at room temperature using 2.5 mol% catalyst loading in 1 h. After each run, an external magnetic field was applied on the outer surface of the glass reaction vessel containing the magnetic nanoparticles using a small permanent magnet. The reaction solution was then easily removed from the reaction vessel by decantation while the external magnet held the basic nanoparticles stationary inside the vessel. The magnetic catalyst was washed with benzene to remove any physisorbed reagents, dried under vacuum at room temperature overnight, and reused in further reactions under identical conditions to the first run. Quantitative conversion was still achieved in the fifth run, with all of the benzaldehyde being converted to the desired product. However, kinetic studies indicated that the catalytic activity of the basic magnetic nanoparticles in the Knoevenagel reaction decreased slightly after one use. In a second experiment where aliquots were sampled during the course of the reaction, 46 and 68% conversions were observed after 20 and 30 min in the second run, while the reaction afforded 59 and 72% conversions after the same reaction time in the first run, respectively. Although it was previously reported that no loss of activity was observed for reused silica supported catalysts in the Knoevenagel reaction [27,36], no kinetic data were provided, and only conversions at the end of the experiment were mentioned. A possible contribution to the deactivation of the catalyst that was observed here may be associated with clustering of the magnetic nanoparticles upon repeated use, reducing the accessibility of the catalytic sites. As mentioned earlier, although a good dispersion of the magnetic nanoparticles in solution was always achieved based on visual inspection, interparticle interactions leading to clustering could still occur to some extent [48].

The study was then extended to the Knoevenagel condensation of several aromatic and heteroaromatic aldehydes with malononitrile using the magnetic base catalyst. Reactions were carried out in benzene at room temperature in 2 h with 1.5 mol% catalyst loading. Results are listed in Table 1. As expected for nucleophilic addition reactions, aromatic aldehydes with electron-withdrawing groups such as nitro ($-\text{NO}_2$) and chloro ($-\text{Cl}$) moieties were more reactive, with complete conversion being achieved (entries 1 and 2). Quantitative conversion was also observed for the reaction of aldehydes containing electron-donating groups such as hydroxyl ($-\text{OH}$), methyl ($-\text{CH}_3$), and methoxy ($-\text{OCH}_3$) (entries 3–5). In the case of hydroxybenzaldehydes, the 2-substituted isomer (entry 6) was found to be slightly less reactive than the 4-substituted isomer, probably due to the increased steric bulk of the 2-substituted isomer. It was previously reported that the reaction rates in Knoevenagel condensations are slowed when bulky reagents were used [50]. For the reaction of aldehyde derivatives of pyridine, the 2-substituted isomer was found to be slightly more reactive than 4-substituted isomer (entries 7 and 8). This could be rationalized based on

Table 1

Knoevenagel reaction of aromatic and heteroaromatic aldehydes with malononitrile using basic magnetic nanoparticle catalyst

Entry	Substrate	Product	Conversion (%)
1			100
2			100
3			100 ^a
4			100
5			100
6			94 ^a
7			100
8			92
9			69
10			71

^a Reaction carried out in benzene:THF = 1:1.

the electron-withdrawing effect (inductive) of the electronegative nitrogen atom. As the inductive effect decreases rapidly with distance [51], the 2-substituted isomer where the carbonyl group is closer to the nitrogen atom would be more reactive towards nucleophilic addition reactions, compared to the 4-substituted isomer. Aldehyde derivatives of pyrrole and furan were found to be much less reactive than other aldehydes in the Knoevenagel condensation with only approximately 70% conversion being observed (entries 9 and 10). Again, in all cases, after the reaction, the magnetic nanoparticle base catalyst was readily separated from the reaction mixture by magnetic decantation.

4. Conclusions

In conclusion, cobalt spinel ferrite magnetic nanoparticles were readily synthesized and functionalized with a diamine

moiety via silane chemistry to create surface basic sites. The basic magnetic nanoparticles were used as efficient heterogeneous catalysts for the Knoevenagel condensation reaction of several aromatic aldehydes with malononitrile under mild conditions. Modification of the acidity of the magnetic nanoparticle support resulted in a significant effect on catalytic activity. It was apparent that the basic magnetic catalyst could be an alternative to amino-functionalized porous silica catalysts for the Knoevenagel reaction, as the initial reaction rate over the magnetic nanoparticles was roughly comparable to the large pore, mesoporous SBA-15 catalysts. The slight decrease in rate over the nanoparticle catalysts was attributed to some nanoparticle clustering in solution, as was suggested by in TEM images. The basic magnetic catalyst could be facilely isolated from the reaction mixture by simple magnetic decantation using a permanent magnet and it could be reused several times without significant degradation in activity. No contribution from homogeneous catalysis by active amine species leaching into reaction solution during the course of the reaction was detected. Our results here demonstrate the feasibility of applying magnetic nanoparticles as catalyst supports for immobilizing simple organic catalysts, giving reaction rates that are comparable to today's benchmark mesoporous silica catalysts.

Acknowledgements

The US DOE Office of Basic Energy Sciences is acknowledged for financial support through Catalysis Science Contract No. DE-FG02-03ER15459. DuPont is also thanked for a Young Professor Award. CSG thanks Dr. Yolande Berta for the TEM images and Mehmet Kutukcu for the XRD pattern.

References

- [1] J.A. Gladysz, *Chem. Rev.* 102 (2002) 3215.
- [2] N.E. Leadbeater, M. Marco, *Chem. Rev.* 102 (2002) 3217.
- [3] D.E.D. Vos, M. Dams, B.F. Sels, P.A. Jacobs, *Chem. Rev.* 102 (2002) 3615.
- [4] A.P. Wight, M.E. Davis, *Chem. Rev.* 102 (2002) 3589.
- [5] B. Cornils, W.A. Herrmann, P. Panster, S. Wieland, *Applied Homogeneous Catalysis with Organometallic Compounds*, Wiley/VCH, Weinheim, 1996, p. 576.
- [6] D. Astruc, F. Lu, J.R. Aranzas, *Angew. Chem. Int. Ed.* 44 (2005) 7852.
- [7] N.T.S. Phan, C.S. Gill, J.V. Nguyen, Z.J. Zhang, C.W. Jones, *Angew. Chem. Int. Ed.* 45 (2006) 2209.
- [8] C. Liu, B. Zou, A.J. Rondinone, Z.J. Zhang, *J. Am. Chem. Soc.* 122 (2000) 6263.
- [9] M.L. Vadala, M.A. Zalich, D.B. Fulks, T.G.S. Pierre, J.P. Dailey, J.S. Riffle, *J. Magn. Magn. Mater.* 239 (2005) 162.
- [10] T.-J. Yoon, W. Lee, Y.-S. Oh, J.-K. Lee, *New J. Chem.* 27 (2003) 227.
- [11] S.C. Tsang, V. Caps, I. Paraskevass, D. Chadwick, D. Thompsett, *Angew. Chem. Int. Ed.* 43 (2004) 5645.
- [12] A.H. Lu, W. Schmidt, N. Matoussevitch, H. Bonnemann, B. Spliethoff, B. Tesche, E. Bill, W. Kiefer, F. Schuth, *Angew. Chem. Int. Ed.* 43 (2004) 4303.
- [13] P.D. Stevens, J. Fan, H.M.R. Gardimalla, M. Yen, Y. Gao, *Org. Lett.* 7 (2005) 2085.
- [14] A. Hu, G.T. Yee, W. Lin, *J. Am. Chem. Soc.* 127 (2005) 12486.
- [15] X. Gao, K.M.K. Yu, K.Y. Tam, S.K. Tsang, *Chem. Commun.* 24 (2003) 2998.
- [16] F. Freeman, *Chem. Rev.* 80 (1981) 329.
- [17] L.F. Tietze, *Chem. Rev.* 96 (1996) 115.
- [18] D.B. Jackson, D.J. Macquarrie, J.H. Clark, in: D.C. Sherrington, A.P. Kybett (Eds.), *Supported Catalysts and their Applications*, RSC, Cambridge, 2001, p. 203.
- [19] D.J. Macquarrie, D.B. Jackson, S. Tailland, K.A. Utting, *J. Mater. Chem.* 11 (2001) 1843.
- [20] I. Rodriguez, S. Iborra, A. Corma, F. Rey, J.L. Jordá, *Chem. Commun.* 7 (1999) 593.
- [21] S. Jaenicke, G.K. Chuah, X.H. Lin, X.C. Hu, *Microporous Mesoporous Mater.* 35 (2000) 143.
- [22] K.S. Kim, J.H. Song, J.H. Kim, G. Seo, *Stud. Surf. Sci. Catal.* 146 (2003) 505.
- [23] Y. Inaki, Y. Kajita, H. Yoshida, K. Ito, T. Hattori, *Chem. Commun.* 22 (2001) 2358.
- [24] K. Narasimharao, M. Hartmann, H.H. Thiel, S. Ernst, *Microporous Mesoporous Mater.* 90 (2006) 377.
- [25] I. Rodriguez, H. Cambon, D. Brunel, M. Lasperas, *J. Mol. Catal. A* 130 (1998) 195.
- [26] Y. Xia, R. Mokaya, *Angew. Chem. Int. Ed.* 42 (2003) 2639.
- [27] Y. Kubota, Y. Nishizaki, H. Ikeya, M. Saeki, T. Hida, S. Kawazu, M. Yoshida, H. Fujii, Y. Sugi, *Microporous Mesoporous Mater.* 70 (2004) 135.
- [28] K. Yamashita, T. Tanaka, M. Hayashi, *Tetrahedron* 61 (2005) 7981.
- [29] A.V. Narsaiah, K. Nagaiyah, *Synth. Commun.* 33 (2003) 3825.
- [30] A.J. Rondinone, A.C.S. Samia, Z.J. Zhang, *J. Phys. Chem. B* 103 (1999) 6876.
- [31] X.C. Shen, X.Z. Fang, Y.H. Zhou, H. Liang, *Chem. Lett.* 33 (2004) 1468.
- [32] J.V. Nguyen, C.W. Jones, *Macromolecules* 37 (2004) 1190.
- [33] K. Schumacher, M. Grun, K.K. Unger, *Microporous Mesoporous Mater.* 27 (1999) 201.
- [34] M. Ma, Y. Zhang, W. Yu, H.Y. Shen, H.Q. Zhang, N. Gu, *Colloids Surf. A* 212 (2003) 219.
- [35] F. Gelman, J. Blum, D. Avnir, *Angew. Chem. Int. Ed.* 40 (2001) 3647.
- [36] B.M. Choudary, M.L. Kantam, P. Sreekanth, T. Bandopadhyay, F. Figueras, A. Tuel, *J. Mol. Catal. A* 142 (1999) 361.
- [37] D. Zhao, Q. Huo, J. Feng, B.F. Chmelka, G.D. Stucky, *J. Am. Chem. Soc.* 120 (1998) 6024.
- [38] K. Yu, M.W. McKittrick, C.W. Jones, *Organometallics* 23 (2004) 4089.
- [39] K. Schumacher, C.F.V. Hohenesche, K.K. Unger, R. Ulrich, A.D. Chesne, U. Wiesner, H.W. Spiess, *Adv. Mater.* 11 (1999) 1194.
- [40] A. Galarneau, H. Cambon, F.D. Renzo, F. Fajula, *Langmuir* 17 (2001) 8328.
- [41] R. Zeng, X. Fu, C. Gong, Y. Sui, X. Ma, X. Yang, *J. Mol. Catal. A* 229 (2005) 1.
- [42] D.J. Macquarrie, J.H. Clark, A. Lambert, J.E.G. Mdoe, A. Priest, *React. Funct. Polym.* 35 (1997) 153.
- [43] G. Langhendries, D.E.D. Vos, G.V. Baron, P.A. Jacobs, *J. Catal.* 187 (1999) 453.
- [44] D.J. Macquarrie, D.B. Jackson, *Chem. Commun.* 18 (1997) 1781.
- [45] J.D. Bass, S.L. Anderson, A. Katz, *Angew. Chem. Int. Ed.* 42 (2003) 5219.
- [46] A. Corma, S. Iborra, I. Rodriguez, F. Sanchez, *J. Catal.* 211 (2002) 208.
- [47] S. Huh, H.T. Chen, J.W. Wiench, M. Pruski, V.S.Y. Lin, *Angew. Chem. Int. Ed.* 44 (2004) 1826.
- [48] C.R. Vestal, Q. Song, Z.J. Zhang, *J. Phys. Chem. B* 108 (2004) 18222.
- [49] U. Wilkenhoner, G. Langhendries, F.V. Laar, G.V. Baron, D.W. Gammon, P.A. Jacobs, E.V. Steen, *J. Catal.* 203 (2001) 201.
- [50] G. Jenner, *Tetrahedron Lett.* 42 (2001) 243.
- [51] L.G. Wade, *Organic Chemistry*, Prentice-Hall, Inc., New Jersey, 1995, p. 945.